AGU ADVANCING EARTH AND SPACE SCIENCES

Geophysical Research Letters

RESEARCH LETTER
10.1029/2023GL106932

Anticyclonic Suppression of the North Pacific Transient Eddy Activity in Midwinter

Satoru Okajima[1], Hisashi Nakamura[1], and Yohai Kaspi[2]

[1]Research Center for Advanced Science and Technology, The University of Tokyo, Tokyo, Japan, [2]Department of Earth and Planetary Sciences, Weizmann Institute of Science, Rehovot, Israel

Key Points:

- Anticyclonic contribution is crucial for the midwinter minimum of the North Pacific transient eddy activity
- This minimum is consistent with net energy loss for anticyclonic regions in midwinter in energy conversion/generation terms
- More attention should be paid to anticyclones in studying midlatitude storm-track activity and their interaction with a time-mean flow

Supporting Information:

Supporting Information may be found in the online version of this article.

Correspondence to:

S. Okajima,
okajima@atmos.rcast.u-tokyo.ac.jp

Citation:

Okajima, S., Nakamura, H., & Kaspi, Y. (2024). Anticyclonic suppression of the North Pacific transient eddy activity in midwinter. *Geophysical Research Letters*, *51*, e2023GL106932. https://doi.org/10.1029/2023GL106932

Received 14 NOV 2023
Accepted 17 JAN 2024

Author Contributions:

Conceptualization: Satoru Okajima, Hisashi Nakamura, Yohai Kaspi
Formal analysis: Satoru Okajima
Funding acquisition: Hisashi Nakamura
Investigation: Satoru Okajima
Methodology: Satoru Okajima
Software: Satoru Okajima
Supervision: Hisashi Nakamura
Writing – original draft: Satoru Okajima
Writing – review & editing: Satoru Okajima, Hisashi Nakamura, Yohai Kaspi

Abstract

Dynamical understandings of midlatitude transient eddy activity, especially its midwinter minimum over the North Pacific, are still limited, partly because conventional Eulerian eddy statistics are incapable of separating cyclonic and anticyclonic contributions. Here we evaluate the two contributions separately based on local curvature of instantaneous flow fields to compare their seasonality between the North Pacific and North Atlantic storm-tracks. The anticyclonic contribution is found crucial for the midwinter minimum of the North Pacific transient eddy activity. Eddy energetics reveals that the net efficiency of the anticyclonic contribution in replenishing total transient eddy energy over the North Pacific exhibits a pronounced midwinter minimum leading to net energy loss, while that of its cyclonic counterpart does not, in harmony with a precipitation peak around midwinter. This study suggests that more attention should be paid to anticyclones in studying midlatitude storm-track dynamics.

Plain Language Summary

Our understanding of the dynamics of midlatitude transient eddy activity, especially its midwinter minimum over the North Pacific, is still limited. This is partly because conventional local statistics based on temporal filtering, which are commonly used as a measure of transient eddy activity, are unable to treat contributions from cyclones and anticyclones separately. Here we evaluate cyclonic and anticyclonic contributions to local eddy statistics separately based on local curvature of instantaneous flow fields, to compare their seasonality between the North Pacific and North Atlantic storm-tracks. The anticyclonic contribution is found crucial for the midwinter minimum of the North Pacific transient eddy activity. We then apply eddy energetics to assess the relative importance of various processes relevant to the seasonality of eddy activity. The net efficiency of the relevant processes associated with the anticyclonic contribution in replenishing total transient eddy energy over the North Pacific exhibits a pronounced midwinter minimum leading to net energy loss. By contrast, that of the cyclonic counterpart does not, in harmony with a precipitation peak around midwinter. This study suggests that more attention should be paid to anticyclones in studying midlatitude storm-track dynamics.

1. Introduction

Midlatitude transient eddies that give rise to day-to-day weather variability are one of the rudimentary components of the Earth's climate system (Hurrell, 1995; Shaw et al., 2016). Blackmon (1976) suggested that regions of large band-pass (with periods of 2–6 days) variance of geopotential height correspond to those of frequent cyclone passage over the North Atlantic (NA) and North Pacific (NP) basins, referring to them as "storm-tracks." Those regions are characterized by prominent lower-tropospheric poleward eddy heat flux (Figure 1) (Blackmon et al., 1977), indicative of baroclinic development of migratory cyclones. Those storm-tracks are collocated with the low-level eddy-driven jets and associated baroclinic zones (Nakamura et al., 2004), and maintained through the effective restoration under the influence of major oceanic frontal zones (Hotta & Nakamura, 2011; Kaspi & Schneider, 2011, 2013).

Eulerian statistics are compatible with quantitative analyses and dynamical diagnostics (Eyring et al., 2021). The eddy energetics is useful for investigating the formation and maintenance mechanisms for the mean westerlies and storm-tracks (Chang et al., 2002; Okajima et al., 2022; hereafter ONK22). Based on Eulerian statistics, the climatological-mean seasonality of storm-track activity, the maintenance mechanisms for the westerly jets and storm-tracks, and their relationship with the lower-boundary condition have been well documented (Chang et al., 2002; Kaspi & Schneider, 2013; Lee & Kim, 2003; Nakamura et al., 2004).

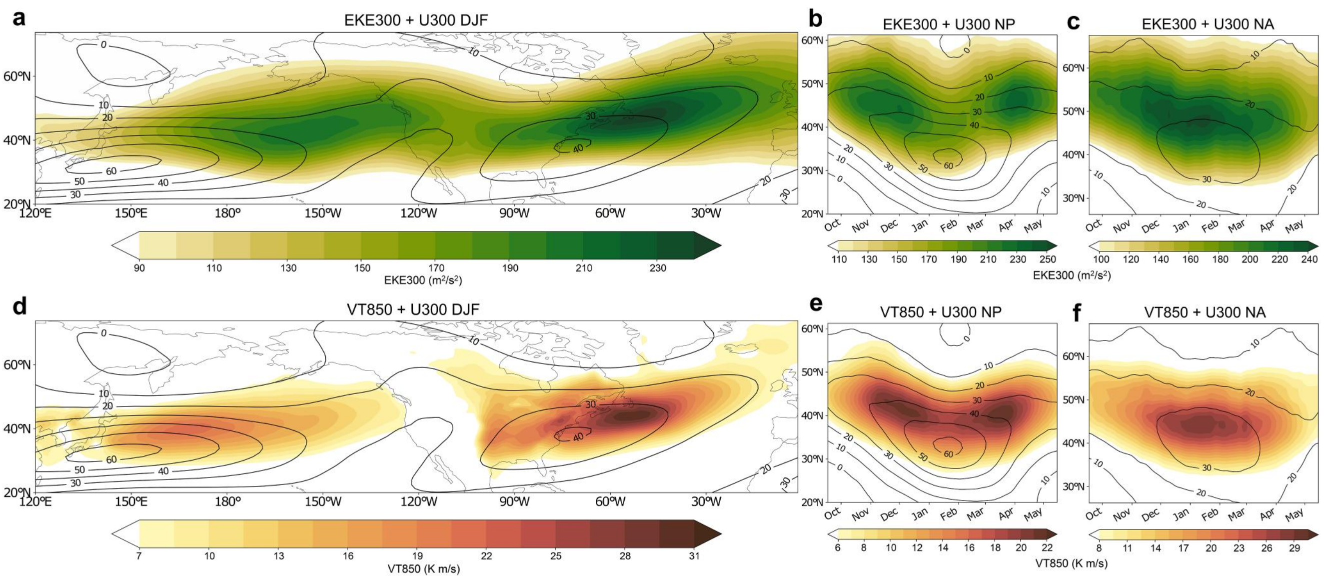

Figure 1. Wintertime climatological-mean transient eddy activity and its seasonality. (a) Climatological-mean wintertime (DJF-mean) EKE_{300} (color, m^2/s^2). Contours denote climatological-mean westerly wind speed (U_{300}; m/s). (b, c) Climatological seasonality in EKE_{300} averaged for 180°−150°W (b) and 60°−30°W (c). Contours denote the corresponding seasonality of U_{300} averaged for 150°E−180° (b) and 70°−40°W (c). A tick mark on the abscissa in b-c represents the first day of a given calendar month. (d–f) Same as in (a–c) respectively, but for $V'T'_{850}$ (color, K m/s), averaged over 150°E−180° (e) and 70°−40°W (f). In this figure and hereafter, the longitudinal sectors for the latitude-season section differ between the lower and upper levels to be consistent with eastward displacement of eddy activity maxima with height.

Nevertheless, dynamical understandings of midlatitude transient eddy activity are still limited, especially for the "midwinter minimum (MWM)" or "midwinter suppression" of the NP transient eddy activity (Nakamura, 1992). Under the maximized upper-level jet speed, the climatological-mean NP transient eddy activity exhibits a clear minimum in midwinter as measured by eddy kinetic energy at 300-hPa (EKE_{300}) (Figure 1b) and poleward eddy heat transport at 850-hPa ($V'T'_{850}$) (Figure 1e). This MWM is inconsistent with the baroclinic instability theory (Eady, 1949) and sharply contrasts with the climatological midwinter maximum of the NA transient eddy activity (Figures 1c and 1f). Various mechanisms have been proposed for this phenomenon, including barotropic (James, 1987) and baroclinic (Schemm & Rivière, 2019) aspects of eddies, diabatic heating (Chang, 2001), trapping of upper-level eddies into the subtropical jet core (Nakamura & Sampe, 2002), an upstream influence (Penny et al., 2010), and structures of the jet streams (Deng & Mak, 2005; Yuval et al., 2018). Based on the comprehensive energetics of transient eddies, ONK22 suggested that multiple processes must be responsible for the MWM. The dynamical origin of the MWM thus remains elusive.

The MWM of the NP transient eddy activity has recently been also investigated through the Lagrangian approach by conducting feature tracking (Hadas & Kaspi, 2021; Schemm & Rivière, 2019). Most of those studies, however, have focused only on migratory cyclones. Okajima et al. (2023; hereafter ONK23) recently revealed that the climatological-mean density of NP surface migratory anticyclones exhibits a clear MWM, while its cyclonic counterpart peaks in midwinter. This suggests that anticyclones are likely key to understanding the mechanisms for the MWM of the NP transient eddy activity. This hypothesis is compatible with the midwinter peak in the climatological-mean precipitation over the NP as well as over the NA (Figure S1 and Text S1 in Supporting Information S1), implying that cyclonic activity may not minimize in midwinter even in the NP.

Therefore, whether anticyclones are indeed important for the MWM of the NP transient eddy activity measured by Eulerian eddy statistics needs to be investigated. However, conventional Eulerian eddy statistics are incapable of separating cyclonic and anticyclonic contributions (Wallace et al., 1988). Recently, a novel method to identify three-dimensional regions of individual cyclonic and anticyclonic rotations was proposed (Okajima et al., 2021; hereafter ONK21). The method enables evaluating cyclonic and anticyclonic contributions separately in Eulerian eddy statistics and atmospheric energetics, as a "hybrid" method into which both Eulerian and Lagrangian perspectives are incorporated.

This study thus aims to give additional insights into the MWM of the NP storm-track activity by unveiling contrasting seasonality of the cyclonic and anticyclonic contributions to transient eddy activity and energetics within the NP and NA storm-tracks. We will demonstrate that anticyclones are more important for the MWM, to argue that more attention should be paid to migratory anticyclones in studying midlatitude storm-track dynamics.

2. Data and Methods

2.1. Atmospheric Reanalysis

We analyze 6-hourly global fields of atmospheric variables, including geopotential height, air temperature, wind velocities, and diabatic heating rates in pressure coordinates, in addition to sea-level pressure, obtained from the Japanese 55-year atmospheric reanalysis (JRA-55) produced by the Japan Meteorological Agency (JMA) (Harada et al., 2016; Kobayashi et al., 2015) for the period 1958–2022. Variables at selected pressure levels are available on a 1.25° × 1.25° grid. At each grid point, fluctuations of a given variable with synoptic-scale transient eddies have been extracted locally from the 6-hourly reanalysis data as its deviations from their low-pass-filtered fields through a 121-point Lanczos filter with a cutoff period of 8 days. Plots showing seasonal evolutions (as in Figure 1) are produced after applying a 31-day running mean to daily climatology.

2.2. Cyclonic and Anticyclonic Contributions to Eulerian Eddy Statistics

Climatological-mean eddy Eulerian statistics are calculated separately for cyclonic and anticyclonic contributions based on two-dimensional local flow curvature κ_2 (ONK21). It is calculated at a given vertical level instantaneously from horizontal winds as

$$\kappa_2 \equiv \frac{1}{R_S} = \frac{1}{V^3}\left(-uvu_x + u^2 v_x - v^2 u_y + uvv_y\right),$$

where R_S denotes the curvature radius, V scaler wind speed, and a subscript denotes zonal or meridional derivative, respectively. A positive (negative) value signifies a cyclonic (anticyclonic) rotation in the Northern Hemisphere. This method effectively removes the effect of shear vorticity associated with the strong westerlies without any temporal filtering to determine the shape of the regions of rotations or vortices. We use unfiltered winds to calculate curvature as in ONK23, who conducted tracking of surface migratory cyclones and anticyclones based on unfiltered SLP. It also helps to retain asymmetry between cyclonic and anticyclonic rotations (e.g., gradient wind balance).

In evaluating Eulerian eddy statistics, the high-pass filtering effectively removes a background field from an instantaneous unfiltered field to highlight signals associated with synoptic-scale features, which are overall consistent with eddies in the unfiltered fields (Figure S2 in Supporting Information S1). Separate contributions from cyclonic and anticyclonic regions to Eulerian statistics are then evaluated by accumulating instantaneous contributions only at grid points where cyclonic or anticyclonic curvature is observed (ONK21), as a practical, ad hoc method (Figure S3 in Supporting Information S1). In this study, the threshold curvatures for cyclonic and anticyclonic rotations are $\pm 3.3 \times 10^{-7}$ m^{-1}, respectively, which are equivalent to a curvature radius of ~3,000 km. It aims to practically remove the effect of planetary-scale waves, which are regarded as part of a background flow for transient eddies. Nevertheless, we have confirmed that results are qualitatively similar when a zero-curvature threshold is used (Figure S4 in Supporting Information S1) or the effect of background planetary-scale waves is eliminated by spectral triangular truncation (subtracting wind fields constructed only by series of spherical harmonics whose degree is less than five ("T4" fields) from the total winds in calculating curvature) (Figure S5 in Supporting Information S1).

2.3. Energetics

The formulation of energetics associated with transient eddy activity follows ONK22. To assess the relative importance of relevant processes independent of eddy amplitude, energy conversion/generation rates are normalized by the total eddy energy as the sum of EKE and EAPE (eddy available potential energy), which is not separated into cyclonic and anticyclonic contributions. The normalized rates are referred to as "*efficiencies*" (Kosaka & Nakamura, 2010; ONK22). The zonally asymmetric climatological-mean state is considered as a background state for high-pass-filtered fluctuations. All the terms related to eddy energy and energy conversion/

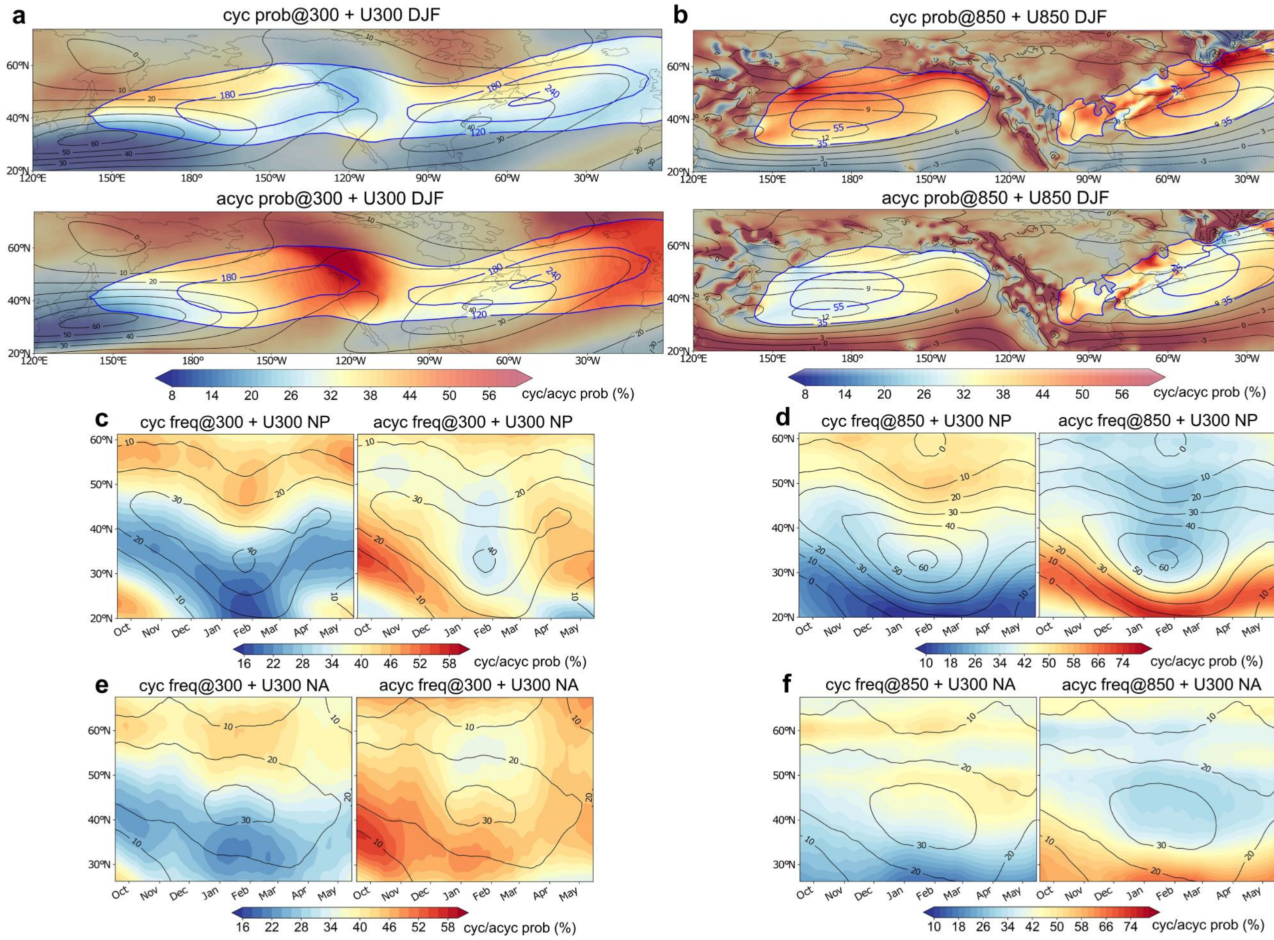

Figure 2. Climatological-mean probability of cyclonic/anticyclonic regions and its seasonality. (a, b) Climatological-mean wintertime (DJF) distributions of probability of cyclonic (upper) and anticyclonic (lower) regions (color, %) at 300-hPa (a) and 850-hPa (b). Black contours denote climatological-mean U_{300} (m/s) (a) and U_{850} (b). Note that the sum of the cyclonic and anticyclonic probabilities does not necessarily equal 1 due to the non-zero curvature threshold. Blue contours signify climatological-mean EKE (m^2/s^2) at 300 hPa (a) and 850 hPa (b). (c) Climatological seasonality in probability of cyclonic (left) and anticyclonic (right) regions (color, %) at 300-hPa averaged for 180°−150°W. Contours denote the corresponding seasonality of U_{300} averaged for 180°−150°W. (d) Same as in (c), but for probability of cyclonic and anticyclonic regions at 850-hPa and U_{300} averaged for 150°E−180°. (e, f) Same as in (c, d) respectively, but for probability of the regions and U_{300} averaged for 70°−40°W (e) and 60°−30°W (f).

generation rates are three-dimensionally integrated over the NP [130°E−130°W, 20°−65°N] or NA [80°−10°W, 25°−65°N] domain from the surface to the 100-hPa level. Energy fluxes are evaluated at the lateral boundaries of those domains (Text S2 and Figure S6 in Supporting Information S1). In this study, energy conversion rates from low-frequency variability to sub-weekly eddies are neglected, because they are only of secondary importance (ONK22).

3. Results

3.1. Probability of Cyclonic and Anticyclonic Regions

In the wintertime (DJF-mean) upper troposphere (Figure 2a), cyclonic regions are more frequently observed north of the jet core region over each of the ocean basins. By contrast, anticyclonic regions are more frequent downstream of a jet core region. Note that those cyclonic and anticyclonic regions are identified through local curvature free from shear vorticity associated with jetstreams. The spatially contrasting probability of cyclonic and anticyclonic regions is common to the two major storm-tracks. In the lower troposphere (Figure 2b), cyclonic regions are more frequent along a low-level eddy-driven jet axis as well as to its north, consistent with results based on cyclone tracking (Hoskins & Hodges, 2002; Shaw et al., 2016; ONK23). The frequent occurrence of low-level

10.1029/2023GL106932

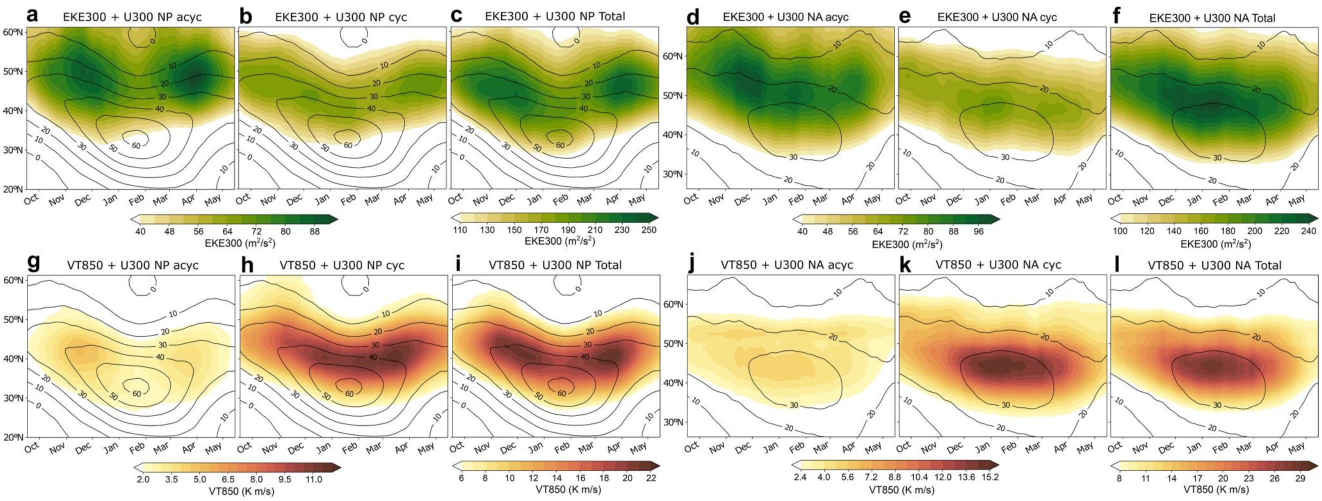

Figure 3. Seasonality of anticyclonic and cyclonic contributions to transient eddy activity. (a, b) Climatological seasonality in EKE_{300} reconstructed only with anticyclonic (a) and cyclonic (b) regions averaged for 180°−150°W. Contours denote the corresponding seasonality of climatological-mean U_{300} averaged for 150°E−180°. (c) Same as in Figure 1b. (d–f) Same as in (a–c) respectively, but for EKE_{300} averaged for 60°−30°W. Contours denote the corresponding seasonality of climatological-mean U_{300} averaged for 70°−40°W. (g–l) Same as in (a–f) respectively, but for $V'T'_{850}$ averaged for 150°E−180° (g–i) and 70°−40°W (j–l).

anticyclonic regions (Figure 2b) is observed along the climatological-mean subtropical high-pressure belt (c.f., Pepler et al., 2019).

The climatological seasonality of the probability of lower-tropospheric cyclonic and anticyclonic regions (Figure 2d) is consistent with the results based on tracking of NP surface migratory cyclones and anticyclones, respectively (ONK23). Over the midwinter NP, the probability of lower-tropospheric cyclonic regions peaks, and its maximum expands equatorward under the strongest, equatorward-shifted Pacific jet. Contrastingly, the anticyclonic counterpart minimizes in midwinter around the storm-track axis near 40°N. The corresponding probability of upper-tropospheric cyclonic curvature exhibits a similar midwinter maximum and equatorward expansion (Figure 2c). In comparison, lower- and upper-tropospheric cyclonic regions over the NA exhibit less obvious seasonality than over the NP, as the NA jet exhibits only modest equatorward displacement and strengthening in midwinter (Figures 2e and 2f).

3.2. Cyclonic and Anticyclonic Contributions to Transient Eddy Activity

Figures 3a–3f show the climatological seasonality of cyclonic and anticyclonic contributions to upper-tropospheric transient eddy activity over the NP and NA, where the latter contribution is overall greater than the former. The anticyclonic contribution to EKE_{300} exhibits a pronounced MWM under the prominent NP jet (Figure 3a), while its cyclonic counterpart does not minimize in midwinter (Figure 3b). The distinct seasonality suggests that the anticyclonic contribution is predominantly responsible for the MWM of the total EKE_{300} (Figures 1b and 3c). In contrast to the NP, the anticyclonic contribution to EKE_{300} over the NA does not exhibit a clear MWM (Figure 3d). Its cyclonic counterpart maximizes in midwinter (Figure 3e). Their contributions correspond to the single peak in EKE_{300} over the NA (Figures 1c and 3f).

The climatological seasonality of cyclonic and anticyclonic contributions to $V'T'_{850}$ also exhibits discernible differences between the NP and NA (Figures 3g–3l), similar to those of EKE_{300}. Although the anticyclonic contribution to $V'T'_{850}$ is overall substantially weaker (<50%) than its cyclonic counterpart as shown by ONK21, only the former exhibits an obvious MWM over the NP as the total $V'T'_{850}$ does (Figures 1e, 3g, and 3i). By contrast, the cyclonic contribution to $V'T'_{50}$ is rather constant throughout the winter with a slight peak in late winter (Figure 3h). This is compatible with the midwinter peak in precipitation over the NP associated with cyclonic regions (Figure S7 in Supporting Information S1). Contrastingly, over the NA, both the cyclonic and anticyclonic contributions to $V'T'_{850}$ exhibit no clear MWM (Figures 3j and 3k), contributing to the single midwinter peak in the total $V'T'_{850}$ (Figures 1f and 3l).

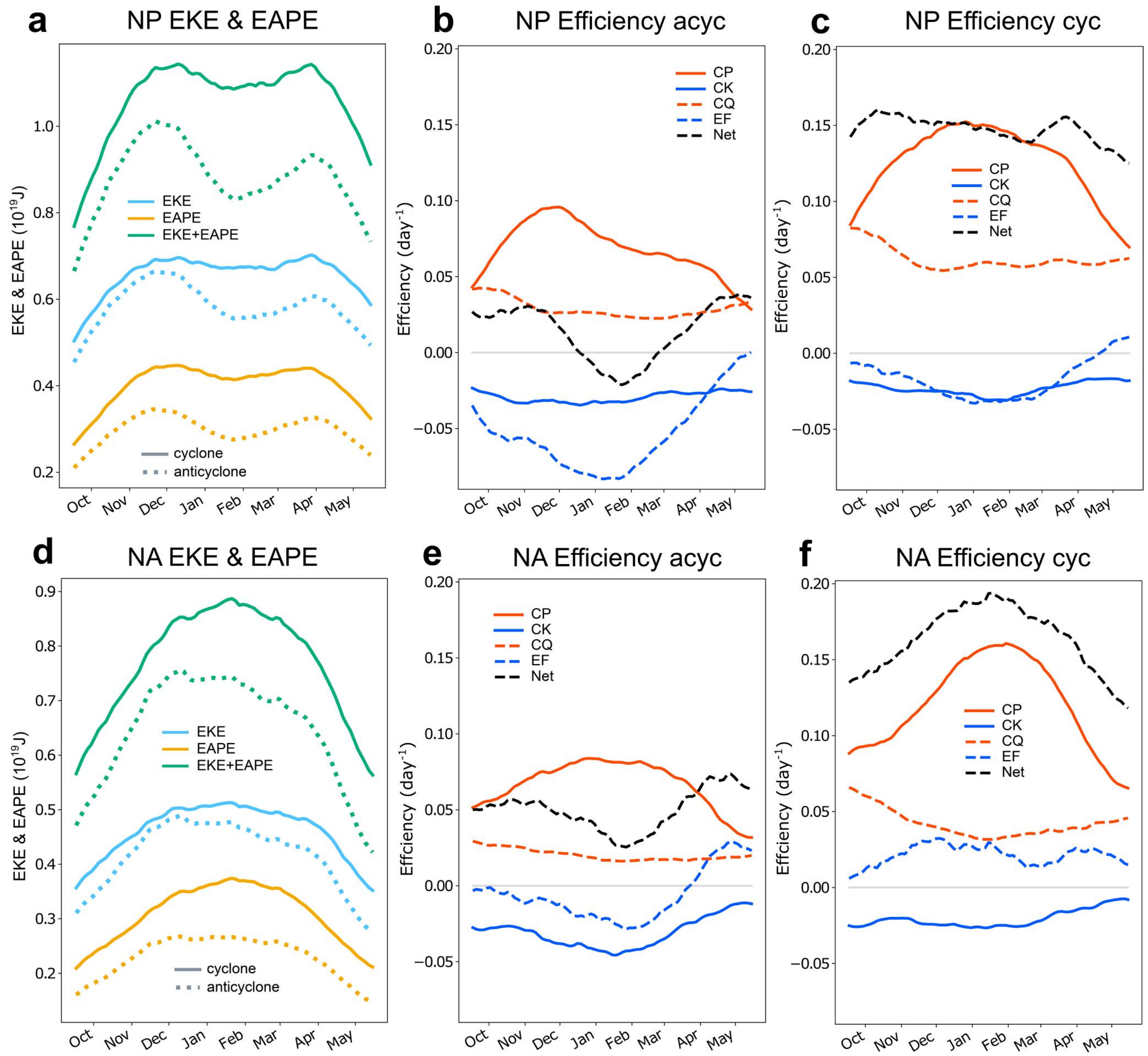

Figure 4. Seasonality in the energetics regarding the anticyclonic and cyclonic contributions. (a) Climatological-mean seasonal evolution of EKE_{3D} (light blue), $EAPE_{3D}$ (orange), and EKE_{3D} + $EAPE_{3D}$ (green) (10^{19}J). All the quantities plotted are integrated three-dimensionally over the NP domain. Solid and dotted lines signify the cyclonic and anticyclonic contributions, respectively. (b, c) Same as in a, but for "efficiency" (day^{-1}) of barotropic energy conversion (CK; blue solid), baroclinic energy conversion (CP; red solid), energy generation through diabatic processes (CQ; red dashed), and horizontal energy flux term (EF; blue dashed) contributed to by anticyclonic (b) and cyclonic regions (c) over the NP domain. Black dashed lines denote the net efficiency relevant to the budget of EKE_{3D} + $EAPE_{3D}$ (viz. CK + CP + CQ + EF). (d–f) Same as in (a–c) respectively, but for the NA domain.

3.3. Energetics

Quantitative evaluation of eddy energetics separately for the cyclonic and anticyclonic contributions can delineate relevant processes for their distinct seasonality. We evaluate the "efficiency" of a given energetic term, whose reciprocal represents the time to replenish the three-dimensionally integrated total eddy energy (EKE_{3D} + $EAPE_{3D}$) over each of the entire NP and NA storm-track domains solely by that term, which is independent of eddy amplitude (ONK22).

Over the NP (Figure 4a), a more distinct MWM is observed for the anticyclonic contribution than for its cyclonic counterpart to each of EKE_{3D}, $EAPE_{3D}$, and EKE_{3D} + $EAPE_{3D}$, which is consistent with the preceding results

(Figure 3). Over the NA (Figure 4d), contrastingly, those three types of eddy energy all peak in early- or mid-winter, regardless of the cyclonic or anticyclonic contribution. For both the NP and NA, the systematically larger cyclonic $EAPE_{3D}$ compared to its anticyclonic counterpart may be an indication of the more baroclinic nature of migratory cyclones.

Over the NP, the net "efficiency" of the energy conversion/generation terms associated with anticyclonic regions exhibits a distinct MWM that is indeed a net energy loss (Figure 4b). This is contributed to mainly by the declining positive efficiency of the baroclinic energy conversion (CP) from early winter and the negative efficiency of the net energy flux term (EF) that is most enhanced in midwinter. This seasonality of the anticyclonic EF term is mainly due to the energy outflux through the eastern boundary and the energy influx through the western boundary (Figure S6a and Text S2 in Supporting Information S1), the latter of which corresponds to the seeding effect from upstream (Penny et al., 2010). By contrast, the net efficiency associated with cyclonic regions over the NP exhibits only a slight minimum in early March (Figure 4c), while systematically higher than its anticyclonic counterpart throughout the cold season. Among the cyclonic contributions evaluated, the CP term exhibits the highest efficiency with the most pronounced peak in early- through mid-winter. The contribution from "neutral" regions between cyclonic and anticyclonic regions to eddy energy does not exhibit a clear MWM, and the net efficiency associated with "neutral" regions peaks in midwinter (Figure S8 in Supporting Information S1).

The anticyclonic contribution to the net efficiency of energy conversion/generation exhibits a well-defined MWM also over the NA (Figure 4e), but unlike over the NP, it is still positive even in midwinter. This MWM is primarily due to the barotropic energy conversion (CK) and EF terms, whose negative contributions maximize in midwinter, acting against the midwinter maximum of the CP efficiency. In midwinter, the energy outflux maximizes, while the energy influx from the upstream minimizes (Figure S6b in Supporting Information S1). In comparison, the net efficiency associated with cyclonic regions exhibits a sharp midwinter maximum over the NA (Figure 4f), due primarily to the pronounced midwinter maximum in the CP efficiency. Unlike its anticyclonic counterpart, the cyclonic EF term is positive and does not minimize in midwinter (Figure 4f). In essence, when compared with the NP storm-track, both the less prominent MWM of the anticyclonic net efficiency and the more prominent midwinter maximum of its cyclonic and "neutral" counterparts (Figure S8 in Supporting Information S1) yield the prominent midwinter peak in the NA eddy activity (Figures 1c, 1f, and 4d).

For both the NP and NA, the efficiency of the total diabatic energy generation (CQ) is positive throughout the cold season with a slight MWM over the NA (Figures 4b, 4c, 4e, and 4f). This is due to a midwinter offset between the maximum generation through precipitation and the maximum damping through air-sea heat exchange represented as the vertical diffusion term (Supplementary Figures S6c, S6d, and Text S2 in Supporting Information S1). This offset is more evident in the cyclonic contribution.

4. Conclusions

Utilizing a novel method for separate identification of cyclonic and anticyclonic regions based on local flow curvature (ONK21), this study demonstrates that the anticyclonic contribution to transient eddy activity plays a pivotal role in setting its MWM over the NP, which cannot be obtained solely through the Lagrangian or Eulerian approach. We thus posit that not only cyclones but also anticyclones need to be considered in investigating transient eddy activity measured as Eulerian eddy statistics, which has been overlooked in previous studies. The importance of anticyclones is compatible with the fact that the MWM of the NP transient eddy activity has been reproduced in Eulerian statistics even in coarse-resolution GCMs (Christoph et al., 1997; Zhang & Held, 1999).

For the contrasting seasonality of cyclonic and anticyclonic contributions to transient eddy activity, their probability is also found important (Figure 2). We, therefore, hypothesize that the MWM of surface migratory anticyclone density over the NP (ONK23) is one of the crucial factors for the MWM of transient eddy activity. An important factor giving rise to the MWM of migratory anticyclone density over the NP, which is unique to the NP storm-track, is midwinter suppression of the genesis of migratory surface anticyclones around the Japan Sea under the intensified monsoonal northwesterlies and equatorward-shifted prominent upper-level jet (ONK23). Another factor is the midwinter maximum of the eddy energy outflux from the eastern NP associated mainly with anticyclonic regions. The tendency for migratory anticyclones to propagate farther downstream compared to cyclones that exhibit a poleward-propagating tendency away from the jet because of diabatic heating (Tamarin & Kaspi, 2016, 2017) may also be relevant.

The seasonality of the net efficiency is still asymmetric between the cyclonic and anticyclonic contributions even after normalized by their probability over the NP and NA (Figure S9 in Supporting Information S1). This suggests that intrinsic cyclone-anticyclone asymmetry may exist regardless of their probability. An intriguing finding is that the net efficiency only of the anticyclonic energy conversion/generation terms exhibits a distinct MWM both over the NP and NA. Potentially relevant factors regarding the asymmetry include diabatic heating, gradient wind balance, and typical moving direction, which will be covered by our future studies. Evaluation of the energy flux between cyclonic and anticyclonic regions also warrants future studies.

It is yet to be understood how the contrasting cyclonic and anticyclonic contributions lead to the MWM as their net effect. Applying the framework used in this study to idealized GCM experiments with zonally symmetric configurations, for example, by Novak et al. (2020) and Yuval et al. (2018) will be informative. The MWM of the NA transient eddy activity under the extremely strong jet years (Afargan & Kaspi, 2017; Montoya Duque et al., 2021) may also be a relevant target for a deeper understanding of the mechanism. The difference between the NP storm-track core region (Figure 3) and its entrance, in which the anticyclonic contribution is still important for the MWM of the total eddy statistics while the cyclonic contribution features a pronounced spring peak in EKE_{300} and equatorward expansion of a spring peak in $V'T'_{850}$, is to be investigated.

Finally, this study suggests that we should consider an anticyclonic contribution in investigating transient eddy activity in the warmed future climate (Eyring et al., 2021; Seneviratne et al., 2021), in which the westerly jet is overall projected to shift or expand poleward. Such investigations have been carried out either by Eulerian eddy statistics (Harvey et al., 2020) or by cyclone tracking (Priestley & Catto, 2022). The "hybrid" perspective would be helpful for a deeper understanding of future changes in storm-track activity.

Data Availability Statement

The JRA-55 reanalysis is from the Data Integration and Analysis System (DIAS; https://search.diasjp.net/en/dataset/JRA55). The GPCP v3.2 monthly precipitation data is from Huffman et al. (2022). Inkscape v1.0.1 (https://inkscape.org/release/1.0.1/) is used to generate the figures.

Acknowledgments
The authors are grateful for sound criticism and useful suggestions by the two anonymous reviewers on the earlier version of this paper. This study is supported in part by the Japanese Ministry of Education, Culture, Sports, Science and Technology (MEXT) through the Arctic Challenge for Sustainability II (ArCS-II; JPMXD1420318865) and the Advanced Studies of Climate Change Projection (SENTAN; JPMXD0722680395), by the Japan Science and Technology Agency through COI-NEXT (JPMJPF2013), by the Environment Research and Technology Development Fund (JPMEERF20222002) of the Environmental Restoration and Conservation Agency of Japan, and by the Japan Society for the Promotion of Science (JSPS) through Grants-in-Aid for Scientific Research 19H05702 (on Innovative Areas 6102), 20H01970, 22H01292, and 22K14097. Y.K. acknowledges support from the JSPS Invitational Fellowship for Research in Japan that supported a sabbatical at the University of Tokyo and ignited this collaboration, for support from the Research Center for Advanced Technology and Science at the University of Tokyo and the Israeli Science Foundation (Grant 996/20).

References

Afargan, H., & Kaspi, Y. (2017). A midwinter minimum in North Atlantic storm track intensity in years of a strong jet. *Geophysical Research Letters*, *44*(24), 12–511. https://doi.org/10.1002/2017gl075136

Blackmon, M. L. (1976). A climatological spectral study of the 500 mb geopotential height of the Northern Hemisphere. *Journal of the Atmospheric Sciences*, *33*(8), 1607–1623. https://doi.org/10.1175/1520-0469(1976)033<1607:acssot>2.0.co;2

Blackmon, M. L., Wallace, J. M., Lau, N.-C., & Mullen, S. L. (1977). An observational study of the Northern Hemisphere wintertime circulation. *Journal of the Atmospheric Sciences*, *34*(7), 1040–1053. https://doi.org/10.1175/1520-0469(1977)034<1040:aosotn>2.0.co;2

Chang, E. K. M. (2001). GCM and observational diagnoses of the seasonal and interannual variations of the Pacific storm track during the cool season. *Journal of the Atmospheric Sciences*, *58*(13), 1784–1800. https://doi.org/10.1175/1520-0469(2001)058<1784:gaodot>2.0.co;2

Chang, E. K. M., Lee, S., & Swanson, K. L. (2002). Storm track dynamics. *Journal of Climate*, *15*(16), 2163–2183. https://doi.org/10.1175/1520-0442(2002)015<02163:std>2.0.co;2

Christoph, M., Ulbrich, U., & Speth, P. (1997). Midwinter suppression of North Hemisphere storm track activity in the real atmosphere and in GCM experiments. *Journal of the Atmospheric Sciences*, *54*(12), 1589–1599. https://doi.org/10.1175/1520-0469(1997)054<1589:msonhs>2.0.co;2

Deng, Y., & Mak, M. (2005). An idealized model study relevant to the dynamics of the midwinter minimum of the Pacific storm track. *Journal of the Atmospheric Sciences*, *62*(4), 1209–1225. https://doi.org/10.1175/jas3400.1

Eady, E. T. (1949). Long waves and cyclone waves. *Tellus*, *1*(3), 33–52. https://doi.org/10.1111/j.2153-3490.1949.tb01265.x

Eyring, V., Gillett, N. P., Achutarao, K., Barimalala, R., Barreiro Parrillo, M., Bellouin, N., et al. (2021). Human influence on the climate system. In V. Masson-Delmotte, P. Zhai, A. Pirani, S. L. Connors, C. Péan, S. Berger, et al. (Eds.), *Climate change 2021: The physical science basis. Contribution of working group I to the sixth assessment report of the intergovernmental panel on climate change* (pp. 423–552). Cambridge University Press.

Hadas, O., & Kaspi, Y. (2021). Suppression of baroclinic eddies by strong jets. *Journal of the Atmospheric Sciences*, *78*(8), 2445–2457. https://doi.org/10.1175/jas-d-20-0289.1

Harada, Y., Kamahori, H., Kobayashi, C., Endo, H., Kobayashi, S., Ota, Y., et al. (2016). The JRA-55 reanalysis: Representation of atmospheric circulation and climate variability. *Journal of the Meteorological Society of Japan*, *94*(3), 269–302. https://doi.org/10.2151/jmsj.2016-015

Harvey, B. J., Cook, P., Shaffrey, L. C., & Schiemann, R. (2020). The response of the Northern Hemisphere storm tracks and jet streams to climate change in the CMIP3, CMIP5, and CMIP6 climate models. *Journal of Geophysical Research*, *125*(23), e2020JD032701. https://doi.org/10.1029/2020jd032701

Hoskins, B. J., & Hodges, K. I. (2002). New perspectives on the Northern Hemisphere winter storm tracks. *Journal of the Atmospheric Sciences*, *59*(6), 1041–1061. https://doi.org/10.1175/1520-0469(2002)059<1041:npotnh>2.0.co;2

Hotta, D., & Nakamura, H. (2011). On the significance of the sensible heat supply from the ocean in the maintenance of the mean baroclinicity along storm tracks. *Journal of Climate*, *24*(13), 3377–3401. https://doi.org/10.1175/2010jcli3910.1

Huffman, G. J., Behrangi, A., Bolvin, D. T., & Nelkin, E. J. (2022). GPCP version 3.2 Satellite-Gauge (SG) combined precipitation data set [Dataset]. Goddard Earth Sciences Data and Information Services Center (GES DISC). https://doi.org/10.5067/MEASURES/GPCP/DATA304

Hurrell, J. W. (1995). Transient eddy forcing of the rotational flow during Northern winter. *Journal of the Atmospheric Sciences*, *52*(12), 2286–2301. https://doi.org/10.1175/1520-0469(1995)052<2286:tefotr>2.0.co;2

James, I. N. (1987). Suppression of baroclinic instability in horizontally sheared flows. *Journal of the Atmospheric Sciences*, *44*(24), 3710–3720. https://doi.org/10.1175/1520-0469(1987)044<3710:sobiih>2.0.co;2

Kaspi, Y., & Schneider, T. (2011). Winter cold of eastern continental boundaries induced by warm ocean waters. *Nature*, *471*(7340), 621–624. https://doi.org/10.1038/nature09924

Kaspi, Y., & Schneider, T. (2013). The role of stationary eddies in shaping midlatitude storm tracks. *Journal of the Atmospheric Sciences*, *70*(8), 2596–2613. https://doi.org/10.1175/jas-d-12-082.1

Kobayashi, S., Ota, Y., Harada, Y., Ebita, A., Moriya, M., Onoda, H., et al. (2015). The JRA-55 reanalysis: General specifications and basic characteristics. *Journal of the Meteorological Society of Japan*, *93*(1), 5–48. https://doi.org/10.2151/jmsj.2015-001

Kosaka, Y., & Nakamura, H. (2010). Mechanisms of meridional teleconnection observed between a summer monsoon system and a subtropical anticyclone. Part I: The Pacific–Japan pattern. *Journal of Climate*, *23*(19), 5085–5108. https://doi.org/10.1175/2010jcli3413.1

Lee, S., & Kim, H.-K. (2003). The dynamical relationship between subtropical and eddy-driven jets. *Journal of the Atmospheric Sciences*, *60*(12), 1490–1503. https://doi.org/10.1175/1520-0469(2003)060<1490:tdrbsa>2.0.co;2

Montoya Duque, E., Lunkeit, F., & Blender, R. (2021). North Atlantic midwinter storm track suppression and the European weather response in ERA5 reanalysis. *Theoretical and Applied Climatology*, *144*(3), 839–845. https://doi.org/10.1007/s00704-021-03517-z

Nakamura, H. (1992). Midwinter suppression of baroclinic wave activity in the Pacific. *Journal of the Atmospheric Sciences*, *49*(17), 1629–1642. https://doi.org/10.1175/1520-0469(1992)049<1629:msobwa>2.0.co;2

Nakamura, H., & Sampe, T. (2002). Trapping of synoptic-scale disturbances into the North-Pacific subtropical jet core in midwinter. *Geophysical Research Letters*, *29*(16), 1–4. https://doi.org/10.1029/2002gl015535

Nakamura, H., Sampe, T., Tanimoto, Y., & Shimpo, A. (2004). Observed associations among storm tracks, jet streams and midlatitude oceanic fronts. Earth's Climate: The Ocean–Atmosphere Interaction. *Geophysical Monograph Series*, *147*, 329–345.

Novak, L., Schneider, T., & Ait-Chaalal, F. (2020). Midwinter suppression of storm tracks in an idealized zonally symmetric setting. *Journal of the Atmospheric Sciences*, *77*(1), 297–313. https://doi.org/10.1175/jas-d-18-0353.1

Okajima, S., Nakamura, H., & Kaspi, Y. (2021). Cyclonic and anticyclonic contributions to atmospheric energetics. *Scientific Reports*, *11*(1), 13202. https://doi.org/10.1038/s41598-021-92548-7

Okajima, S., Nakamura, H., & Kaspi, Y. (2022). Energetics of transient eddies related to the midwinter minimum of the North Pacific storm-track activity. *Journal of Climate*, *35*(4), 1137–1156. https://doi.org/10.1175/jcli-d-21-0123.1

Okajima, S., Nakamura, H., & Kaspi, Y. (2023). Distinct roles of cyclones and anticyclones in setting the midwinter minimum of the North Pacific eddy activity: A Lagrangian perspective. *Journal of Climate*, *36*(14), 4793–4814. https://doi.org/10.1175/jcli-d-22-0474.1

Penny, S., Roe, G. H., & Battisti, D. S. (2010). The source of the midwinter suppression in storminess over the North Pacific. *Journal of Climate*, *23*(3), 634–648. https://doi.org/10.1175/2009jcli2904.1

Pepler, A., Dowdy, A., & Hope, P. (2019). A global climatology of surface anticyclones, their variability, associated drivers and long-term trends. *Climate Dynamics*, *52*(9–10), 5397–5412. https://doi.org/10.1007/s00382-018-4451-5

Priestley, M. D. K., & Catto, J. L. (2022). Future changes in the extratropical storm tracks and cyclone intensity, wind speed, and structure. *Weather and Climate Dynamics*, *3*(1), 337–360. https://doi.org/10.5194/wcd-3-337-2022

Schemm, S., & Rivière, G. (2019). On the efficiency of baroclinic eddy growth and how it reduces the North Pacific storm-track intensity in midwinter. *Journal of Climate*, *32*(23), 8373–8398. https://doi.org/10.1175/jcli-d-19-0115.1

Seneviratne, S. I., Zhang, X., Adnan, M., Badi, W., Dereczynski, C., Di Luca, A., et al. (2021). Weather and climate extreme events in a changing climate. In V. Masson-Delmotte, P. Zhai, A. Pirani, S. L. Connors, C. Péan, S. Berger, et al. (Eds.), *Climate change 2021: The physical science basis. Contribution of working group I to the sixth assessment report of the intergovernmental panel on climate change* (pp. 1513–1766). Cambridge University Press.

Shaw, T. A., Baldwin, M., Barnes, E. A., Caballero, R., Garfinkel, C. I., Hwang, Y.-T., et al. (2016). Storm track processes and the opposing influences of climate change. *Nature Geoscience*, *9*(9), 656–664. https://doi.org/10.1038/ngeo2783

Tamarin, T., & Kaspi, Y. (2016). The poleward motion of extratropical cyclones from a potential vorticity tendency analysis. *Journal of the Atmospheric Sciences*, *73*(4), 1687–1707. https://doi.org/10.1175/jas-d-15-0168.1

Tamarin, T., & Kaspi, Y. (2017). The poleward shift of storm tracks under global warming: A Lagrangian perspective. *Geophysical Research Letters*, *44*(20), 10666–10674. https://doi.org/10.1002/2017gl073633

Wallace, J. M., Lim, G.-H., & Blackmon, M. L. (1988). Relationship between cyclone tracks, anticyclone tracks and baroclinic waveguides. *Journal of the Atmospheric Sciences*, *45*(3), 439–462. https://doi.org/10.1175/1520-0469(1988)045<0439:rbctat>2.0.co;2

Yuval, J., Afargan, H., & Kaspi, Y. (2018). The relation between the seasonal changes in jet characteristics and the pacific midwinter minimum in eddy activity. *Geophysical Research Letters*, *45*(18), 9995–10002. https://doi.org/10.1029/2018gl078678

Zhang, Y., & Held, I. M. (1999). A linear stochastic model of a GCM's midlatitude storm tracks. *Journal of the Atmospheric Sciences*, *56*(19), 3416–3435. https://doi.org/10.1175/1520-0469(1999)056<3416:alsmoa>2.0.co;2